

Monophoton signals in light gravitino production at e^+e^- colliders

Kentarou Mawatari^a, Bettina Oehl

Theoretische Natuurkunde and IIHE/ELEM, Vrije Universiteit Brussel,
and International Solvay Institutes, Pleinlaan 2, B-1050 Brussels, Belgium

Abstract. We revisit the monophoton plus missing energy signature at e^+e^- colliders in supersymmetric (SUSY) models where the gravitino is very light. There are two possible processes which provide the signal: gravitino pair production and associated gravitino production with a neutralino, leading the monophoton final state via an additional photon radiation and via the neutralino decay, respectively. By using the superspace formalism, we construct a model that allows us to study the parameter space for the both processes. We show that the signal cross section and the photon spectra provide information on the masses of the SUSY particles as well as the SUSY breaking scale.

1 Introduction

Monophoton events with missing energy ($\gamma + \cancel{E}$) are one of the promising search channels to find new physics at both lepton and hadron colliders. So far no significant signal excess over the Standard Model (SM) background has been observed at the LEP [1–4] as well as at the Tevatron [5–7] and the LHC [8, 9], constraining various kinds of models, e.g. supersymmetry (SUSY) and extra dimensions.

The monophoton signal in the context of SUSY models has been searched for models where the gravitino is the lightest SUSY particle (LSP) with the very light mass $m_{3/2} \sim \mathcal{O}(10^{-14} - 10^{-12} \text{ GeV})$ at the LEP [1–4] and the Tevatron [5].¹ In such scenarios there are two possible processes providing the signal: *gravitino pair production* ($\tilde{G}\tilde{G}$) and *neutralino-gravitino associated production* ($\tilde{\chi}\tilde{G}$). The former leads the monophoton final state via an additional photon radiation, while the latter via the subsequent neutralino decay into a photon and a LSP gravitino.

The $\tilde{\chi}\tilde{G}$ associated production has been studied rather in details [12–17], while the $\tilde{G}\tilde{G}(+\gamma)$ production has been investigated only in models where all SUSY particles except for the gravitino are too heavy to be produced on-shell [18–20].

For the last few years simulation tools in the FEYNRULES [21–23] and MADGRAPH [24, 25] frameworks for processes involving gravitinos/goldstinos have been intensively developed [26–28], making phenomenological studies easier [17, 29–33]. It should be noted, however, that all the above recent studies (except [28]) rely on the effective gravitino Lagrangian that contains only interactions with a single gravitino. To study the $\tilde{G}\tilde{G}$ production, we need

a consistent implementation of all the relevant interactions including vertices involving two gravitinos as well as sgoldstinos, which are the superpartners of goldstinos and play an important role for the unitarity [34, 35]. We also note that the process contains a four-fermion interaction involving two Majorana particles, which is not supported in the default MADGRAPH, and therefore special implementations are required.

In this article, we consider a scenario where the gravitino is the LSP and the lightest neutralino is the next-to-lightest SUSY particle (NLSP) and promptly decays into a photon and a gravitino. We revisit the monophoton plus missing energy signature for future e^+e^- colliders

$$e^+e^- \rightarrow \gamma\tilde{G}\tilde{G} \rightarrow \gamma + \cancel{E}, \quad (1)$$

where, as mentioned, the $\tilde{G}\tilde{G}$ and $\tilde{\chi}\tilde{G}$ productions can be the dominant subprocesses. In order to study the whole parameter space for the both processes, including all the relevant SUSY particles as well as sgoldstinos, we construct a simple SUSY QED model with a goldstino multiplet in the gravitino-goldstino equivalence limit by using the superspace formalism. We investigate the $e^+e^- \rightarrow \tilde{G}\tilde{G}$ process in detail to see how the cross section deviates from that in models where all SUSY particles except for the gravitino are assumed to be heavy and integrated out. We generate the signal samples as well as the SM background, and analyze the signal cross sections and the photon spectra to extract information on the masses of the neutralino and selectrons as well as the gravitino mass, which is related to the SUSY breaking scale.

We note in passing that, although our study in this article focuses on lepton colliders, all the results are applicable for $\gamma + \cancel{E}$ as well as jet + \cancel{E} signals at hadron colliders and the detailed study will be reported elsewhere.

The paper is organized as follows: In Sect. 2 we construct a SUSY QED model including interactions with (s)goldstinos in the superspace formalism. In Sect. 3, we

^a e-mail: kentarou.mawatari@vub.ac.be

¹ A similar light-gravitino scenario has been studied in the monojet plus missing energy signature ($j + \cancel{E}$) at the Tevatron [10] and the LHC [11].

explore the parameter space in the $e^+e^- \rightarrow \tilde{G}\tilde{G}$ process, and briefly review the $e^+e^- \rightarrow \tilde{\chi}\tilde{G}$ process. In Sect. 4, we simulate the $e^+e^- \rightarrow \gamma\tilde{G}\tilde{G}$ process as well as the SM background, and show that the signal cross sections and the photon spectra provide information on the masses of the neutralino and selectrons as well as the gravitino mass. Sect. 5 is devoted to our summary. In Appendix A we give the relevant Lagrangian in terms of the component fields. In Appendix B, to validate our model implementation of sgoldstinos, we briefly discuss the $\gamma\gamma \rightarrow \tilde{G}\tilde{G}$ process.

2 SUSY QED with a goldstino superfield

In phenomenologically viable SUSY models, the SUSY breaking is usually assumed to happen in a so-called hidden sector and then being transmitted to the visible sector (i.e. the SM particles and their superpartners) through some mediation mechanism. As a result, one obtains effective couplings of the fields in the visible sector to the goldstino multiplet. To illustrate the interactions among the physical degrees of freedom of the goldstino multiplet and the fields in the visible sector, we discuss an R -parity conserving $N = 1$ global supersymmetric model with the $U(1)_{\text{em}}$ gauge group in the superspace formalism. The model comprises one vector superfield $V = (A^\mu, \lambda, D_V)$, describing a photon A^μ and a photino λ , and two chiral superfields $\Phi_L = (\tilde{e}_L, e_L, F_L)$ and $\Phi_R = (\tilde{e}_R^*, e_R^c, F_R)$, containing the left- and right-handed electrons $e_{L/R}$ and selectrons $\tilde{e}_{L/R}$. In addition, we introduce a chiral superfield in the hidden sector $X = (\phi, \tilde{G}, F_X)$, containing a sgoldstino ϕ and a goldstino \tilde{G} . D_V , $F_{L/R}$ and F_X are auxiliary fields.

The Lagrangian of the visible sector is

$$\mathcal{L}_{\text{vis}} = \sum_{i=L,R} \int d^4\theta \Phi_i^\dagger e^{2g_e Q_i V} \Phi_i + \frac{1}{4} \left(\int d^2\theta W^\alpha W_\alpha + \text{h.c.} \right), \quad (2)$$

where $g_e = \sqrt{4\pi\alpha}$ and Q_i is the electric charge of Φ_i , i.e. $Q_{R/L} = \pm 1$.² $W_\alpha = -\frac{1}{4}\bar{D}\cdot\bar{D}D_\alpha V$ denotes the SUSY $U(1)_{\text{em}}$ field strength tensor with D being the superderivative. \mathcal{L}_{vis} contains the kinetic terms as well as the gauge interactions.

The Lagrangian of the goldstino superfield is given by

$$\mathcal{L}_X = \int d^4\theta X^\dagger X - \left(F \int d^2\theta X + \text{h.c.} \right) - \frac{c_X}{4} \int d^4\theta (X^\dagger X)^2. \quad (3)$$

The first term gives the kinetic term of the (s)goldstino, while the second term is a source of SUSY breaking and $F \equiv \langle F_X \rangle$ is a vacuum expectation value (VEV) of F_X .³

² The covariant derivative is defined as $D_\mu = \partial_\mu + ig_e Q A_\mu$.

³ Note that we follow the FEYNRULES convention for chiral superfields $\Phi(y, \theta) = \phi(y) + \sqrt{2}\theta \cdot \psi(y) - \theta \cdot \theta F(y)$ [23], which fixes the sign of the Lagrangian so as to give a positive contribution to the scalar potential.

The last term is non-renormalizable and provides interactions between the goldstino multiplet. This term also gives the sgoldstino mass term when replacing the auxiliary fields F_X by the VEV, and hence we assign $c_X = m_\phi^2/F^2$.

The interactions among the (s)goldstinos and the fields in the visible sector as well as the soft mass terms for the selectrons and the photino are given by the effective Lagrangian

$$\mathcal{L}_{\text{int}} = - \sum_{i=L,R} c_{\Phi_i} \int d^4\theta X^\dagger X \Phi_i^\dagger \Phi_i - \left(\frac{c_V}{4} \int d^2\theta X W^\alpha W_\alpha + \text{h.c.} \right), \quad (4)$$

where we identify $c_{\Phi_i} = m_{\tilde{e}_i}^2/F^2$ and $c_V = 2m_\lambda/F$.

We note that our model is minimal, yet enough to investigate the $\gamma + \cancel{E}$ signal at e^+e^- colliders. We also note that our Lagrangian is model independent. However, studies of non-linear SUSY revealed that additional model dependent terms for four-point effective interactions involving two goldstinos and two matter fermions are allowed [36–38]. One possible source for such terms is D -type SUSY breaking [39], which does not occur in our model.

Before turning to collider phenomenology, we briefly refer to the goldstino equivalence theorem. When the global SUSY is promoted to the local one, the goldstino is absorbed by the gravitino via the super-Higgs mechanism. In the high-energy limit, $\sqrt{s} \gg m_{3/2}$, which is always fulfilled for very light gravitinos at colliders, the interactions of the helicity 1/2 components are dominant, and can be well described by the goldstino interactions due to the graviton-goldstino equivalence theorem [40, 41]. We also note that, as a consequence of the super-Higgs mechanism, the gravitino mass is related to the scale of the SUSY breaking and the Planck scale, in a flat space-time, as [42, 43]

$$m_{3/2} = \frac{F}{\sqrt{3} \overline{M}_{\text{Pl}}}, \quad (5)$$

where $\overline{M}_{\text{Pl}} \equiv M_{\text{Pl}}/\sqrt{8\pi} \approx 2.4 \times 10^{18}$ GeV is the reduced Planck mass. Therefore, low-scale SUSY breaking scenarios provide a gravitino LSP. In the following, we simply call the goldstino the gravitino and also call the photino the (lightest) neutralino $\tilde{\chi}$. We note that by construction we ignore other neutralino mixing scenarios. Since the zino and higgsino mixing gives rise to the Z and H decay modes of the neutralino [44], the overall $\gamma + \cancel{E}$ rate decreases, but the property of the signal does not change. The extension of our model to the SM gauge group is straightforward to study the general minimal supersymmetric SM (MSSM); see e.g. [45].

For completeness, we show the relevant interaction Lagrangians of (2), (3) and (4) in terms of the component fields in Appendix A. We have implemented the above Lagrangian by using the superspace module into FEYNRULES 2 [23], which provides the Feynman rules in terms of the physical component fields and the UFO model

file [46, 47] for matrix-element generators such as MADGRAPH 5 [25].

3 Light gravitino production at e^+e^- colliders

Based on the model we constructed in the previous section, we investigate direct LSP gravitino production processes that lead to $\gamma + \cancel{E}$ at future e^+e^- colliders. We consider the neutralino to be the NLSP and to promptly decay into a photon and a gravitino. The missing energy will be carried away by two gravitinos due to the R -parity conservation. Two distinct processes give rise to the signal: *gravitino pair production* ($\tilde{G}\tilde{G}$) and *neutralino-gravitino associated production* ($\tilde{\chi}\tilde{G}$), leading the monophoton final state via an additional photon radiation and via the subsequent neutralino decay, respectively. Their relative importance varies with the gravitino and neutralino masses as well as with kinematical cuts. In the following, a detailed discussion of the $\tilde{G}\tilde{G}$ production is presented, followed by a short review of the $\tilde{\chi}\tilde{G}$ production. According to the cross sections, we fix the benchmark points for our simulation in the next section. We also comment on the validation of our model implementation in the last part of this section.

3.1 Gravitino pair production

Gravitino pair production gives rise to the monophoton plus missing energy signature when an additional photon is emitted [18, 19]. Here we present the helicity amplitudes explicitly for the two-to-two process

$$e^-\left(p_1, \frac{\lambda_1}{2}\right) + e^+\left(p_2, \frac{\lambda_2}{2}\right) \rightarrow \tilde{G}\left(p_3, \frac{\lambda_3}{2}\right) + \tilde{G}\left(p_4, \frac{\lambda_4}{2}\right), \quad (6)$$

where the four momenta (p_i) and helicities ($\lambda_i = \pm 1$) are defined in the center-of-mass (CM) frame of the e^+e^- collision. In the massless limit of e^\pm , one can find that all amplitudes are zero when both the electron and the positron have the same helicity, and hence we fix $\lambda_2 = -\lambda_1$. The same helicity relation holds for the massless gravitinos in the final state, leading to $\lambda_4 = -\lambda_3$. Since we will assume gravitinos with mass $m_{3/2} \sim \mathcal{O}(10^{-13} \text{ GeV})$, we neglect the gravitino mass in the phase space but keep it in the couplings. In addition, for the $\lambda_1 = +1$ ($\lambda_1 = -1$), only right-handed (left-handed) selectrons can contribute to the total amplitudes. Therefore, the helicity amplitudes for the above process can be expressed as the sum of the four-point contact amplitude and the t, u -channel selectron exchange amplitudes (see also Fig. 1):

$$\mathcal{M}_{\lambda_1, \lambda_3} = \mathcal{M}_{\lambda_1, \lambda_3}^c + \mathcal{M}_{\lambda_1, \lambda_3}^t + \mathcal{M}_{\lambda_1, \lambda_3}^u. \quad (7)$$

Using the straightforward Feynman rules for Majorana fermions given in [48], the above amplitudes are writ-

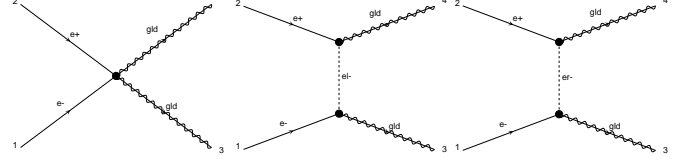


Fig. 1. Samples of Feynman diagrams for gravitino pair production in e^+e^- collisions, generated by (modified) MADGRAPH 5 [25]. **gld**, **el**, and **er** denote a gravitino, a left-handed selectron, and a right-handed selectron, respectively.

ten, based on the effective gravitino Lagrangian in Appendix A, as

$$i\mathcal{M}_{\lambda_1, \lambda_3}^c = -\frac{im_{\tilde{e}_{\lambda_1}}^2}{F^2}(\hat{\mathcal{M}}_{\lambda_1, \lambda_3}^t - \hat{\mathcal{M}}_{\lambda_1, \lambda_3}^u), \quad (8)$$

$$i\mathcal{M}_{\lambda_1, \lambda_3}^t = -\frac{im_{\tilde{e}_{\lambda_1}}^4}{F^2(t - m_{\tilde{e}_{\lambda_1}}^2)}\hat{\mathcal{M}}_{\lambda_1, \lambda_3}^t, \quad (9)$$

$$i\mathcal{M}_{\lambda_1, \lambda_3}^u = \frac{im_{\tilde{e}_{\lambda_1}}^4}{F^2(u - m_{\tilde{e}_{\lambda_1}}^2)}\hat{\mathcal{M}}_{\lambda_1, \lambda_3}^u, \quad (10)$$

where $m_{\tilde{e}_\pm}$ denotes the right/left-handed selectron mass for notational convenience. The reduced helicity amplitudes are

$$\begin{aligned} \hat{\mathcal{M}}_{\lambda_1, \lambda_3}^t &= \bar{u}(p_3, \lambda_3)P_{\lambda_1}u(p_1, \lambda_1) \\ &\quad \times \bar{v}(p_2, -\lambda_1)P_{-\lambda_1}v(p_4, -\lambda_3), \\ \hat{\mathcal{M}}_{\lambda_1, \lambda_3}^u &= \bar{u}(p_4, -\lambda_3)P_{\lambda_1}u(p_1, \lambda_1) \\ &\quad \times \bar{v}(p_2, -\lambda_1)P_{-\lambda_1}v(p_3, \lambda_3), \end{aligned} \quad (11)$$

where $P_\pm = \frac{1}{2}(1 \pm \gamma^5)$ is the chiral projection operator.

With the four momenta defined as

$$\begin{aligned} p_1^\mu &= \frac{\sqrt{s}}{2}(1, 0, 0, 1), \\ p_2^\mu &= \frac{\sqrt{s}}{2}(1, 0, 0, -1), \\ p_3^\mu &= \frac{\sqrt{s}}{2}(1, \sin\theta, 0, \cos\theta), \\ p_4^\mu &= \frac{\sqrt{s}}{2}(1, -\sin\theta, 0, -\cos\theta), \end{aligned} \quad (12)$$

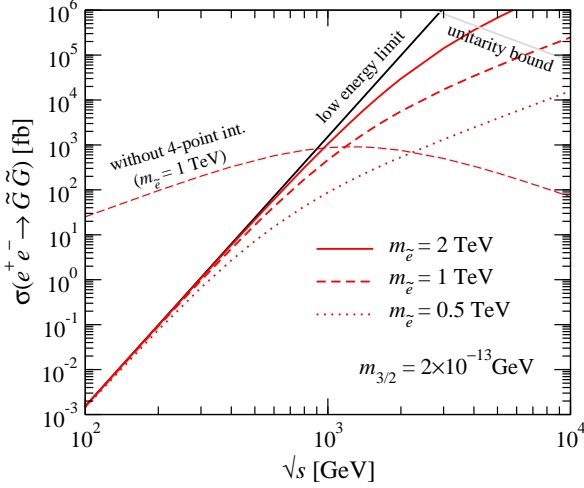
we present the helicity amplitudes in Table 1. The total cross section is given by

$$\begin{aligned} \sigma &= \frac{1}{192\pi F^4} \sum_{\lambda=\pm} \frac{m_{\tilde{e}_\lambda}^4}{s^2} \left[s^3 - 3m_{\tilde{e}_\lambda}^2 s^2 + 9m_{\tilde{e}_\lambda}^4 s \right. \\ &\quad \left. + 3m_{\tilde{e}_\lambda}^6 \left(1 - \frac{m_{\tilde{e}_\lambda}^2}{s + m_{\tilde{e}_\lambda}^2} + 4 \log \frac{m_{\tilde{e}_\lambda}^2}{s + m_{\tilde{e}_\lambda}^2} \right) \right]. \end{aligned} \quad (13)$$

Figure 2 shows the total cross sections as a function of the CM energy \sqrt{s} for three different selectron masses $m_{\tilde{e}_\pm} = 0.5, 1$ and 2 TeV . The gravitino mass is fixed at $m_{3/2} = 2 \times 10^{-13} \text{ GeV}$, which corresponds by (5) to the SUSY breaking scale $\sqrt{F} \approx 918 \text{ GeV}$. We stress that the cross

Table 1. The helicity amplitudes $\mathcal{M}_{\lambda_1, \lambda_3}$ defined in (7) for $e_{\lambda_1}^- e_{-\lambda_1}^+ \rightarrow \tilde{G}_{\lambda_3} \tilde{G}_{-\lambda_3}$.

$\lambda_1 \lambda_3$		\mathcal{M}^c	\mathcal{M}^t	\mathcal{M}^u
$\pm \mp$	$-\frac{s m_{\tilde{e}_{\lambda_1}}^2}{2F^2} (1 - \cos \theta)$	$\left[\begin{array}{c} 1 \\ + \frac{m_{\tilde{e}_{\lambda_1}}^2}{t - m_{\tilde{e}_{\lambda_1}}^2} \end{array} \right]$		
$\pm \pm$	$-\frac{s m_{\tilde{e}_{\lambda_1}}^2}{2F^2} (1 + \cos \theta)$	$\left[\begin{array}{c} 1 \\ + \frac{m_{\tilde{e}_{\lambda_1}}^2}{u - m_{\tilde{e}_{\lambda_1}}^2} \end{array} \right]$		

**Fig. 2.** Total cross sections of $e^+e^- \rightarrow \tilde{G}\tilde{G}$ as a function of the collision energy for different selectron masses $m_{\tilde{e}_{\pm}} = 0.5, 1, 2$ TeV with $m_{3/2} = 2 \times 10^{-13}$ GeV. The cross section in the low-energy limit is presented by a black solid line. The contribution without the four-point interaction for $m_{\tilde{e}_{\pm}} = 1$ TeV is also shown as a reference.

section is extremely sensitive to the gravitino mass since it scales inversely proportionally to the gravitino mass to the fourth,

$$\sigma(\tilde{G}\tilde{G}) \propto 1/m_{3/2}^4. \quad (14)$$

We also note that the cross section tends to be larger for the heavier selectrons since the couplings are proportional to $m_{\tilde{e}}^2$.

In the low-energy limit, $\sqrt{s} \ll m_{\tilde{e}_{\pm}}$, as one can easily see from the explicit amplitudes in Table 1, a strong cancellation happens between \mathcal{M}^c and $\mathcal{M}^{t,u}$, leading to a cross section scaling as [19, 37]

$$\sigma = \frac{s^3}{160\pi F^4}, \quad (15)$$

presented by a black line in Fig. 2. The contribution without the four-point amplitude is also shown as a reference, where one can see the effect of the huge cancellation. It should be noted here that the low-energy limit, which is always assumed in the previous studies [18, 19, 49, 50], may not be a good approximation for future colliders since the selectron masses should be less or of the order of the SUSY breaking scale and might be within the reach of the CM energies. Therefore, one should consider the full expression of the cross section. Figure 2 indeed shows that, as

\sqrt{s} is increasing, the effect of the selectron mass becomes significant. When the CM energy is bigger than the selectron mass, $\sqrt{s} > m_{\tilde{e}}$, the contribution from \mathcal{M}^c becomes more important than that from $\mathcal{M}^{t,u}$. We note that the current gravitino mass bound by the $\tilde{G}\tilde{G}(+\gamma)$ production could weaken if the selectrons are light enough.

Finally, we briefly discuss the unitarity bound. The projected partial wave amplitude is given by

$$\mathcal{J}_{\lambda_1, \lambda_3}^J = \frac{1}{32\pi} \int_{-1}^1 d\cos\theta d_{\lambda_1, \lambda_3}^J(\theta) \mathcal{M}_{\lambda_1, \lambda_3} \quad (16)$$

with the Wigner d -function. Unitarity requires the lowest non-vanishing partial wave to be $|\mathcal{J}_{\lambda_1, \lambda_3}^{J=1}| < 1/2$, leading to the upper bound of the cross section, which is shown by a gray line in Fig. 2. One can see that the lighter selectrons remedy the bad unitarity behavior. It should also be noted that, since we consider the effective model which is valid up to m_{SUSY}/F , a higher energy requires a higher SUSY breaking scale (i.e. a heavier gravitino) or lighter SUSY particles for reliable predictions.

3.2 Neutralino-gravitino associated production

Gravitino production in association with a neutralino and the subsequent neutralino decay,

$$e^+e^- \rightarrow \tilde{\chi}\tilde{G} \rightarrow \gamma\tilde{G}\tilde{G}, \quad (17)$$

leads to the $\gamma + \cancel{E}$ signal already at the leading order [12–17].⁴ We refer to the recent study [17] for a detailed discussion.

Here, we briefly point out two important features of this process. First, unlike the gravitino pair production (14), the total cross section is inversely proportional to the square of the gravitino mass

$$\sigma(\tilde{\chi}\tilde{G}) \propto 1/m_{3/2}^2, \quad (18)$$

as seen in the left plot in Fig. 4, and hence the sensitivity to the gravitino mass is weaker than in the $\tilde{G}\tilde{G}$ production. The cross section depends also on the t, u -channel exchange selectron masses, and increases for the heavier selectrons as in the $\tilde{G}\tilde{G}$ production.

Second, since the $\tilde{\chi} \rightarrow \gamma\tilde{G}$ decay is isotropic, the photon distribution is given by purely kinematical effects of

⁴ The monophoton signal of $\tilde{\chi}\tilde{G}$ production via the Higgs decay at the LHC was studied in [51].

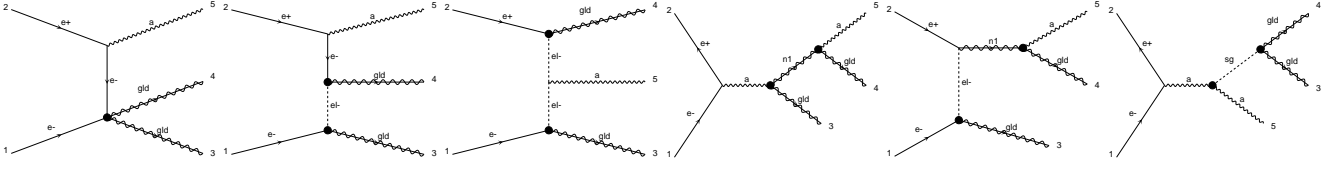


Fig. 3. Representative Feynman diagrams for $e^+e^- \rightarrow \tilde{G}\tilde{G}\gamma$, generated by (modified) MADGRAPH 5 [25]. **n1** and **sg** denote a neutralino and a goldstino, respectively.

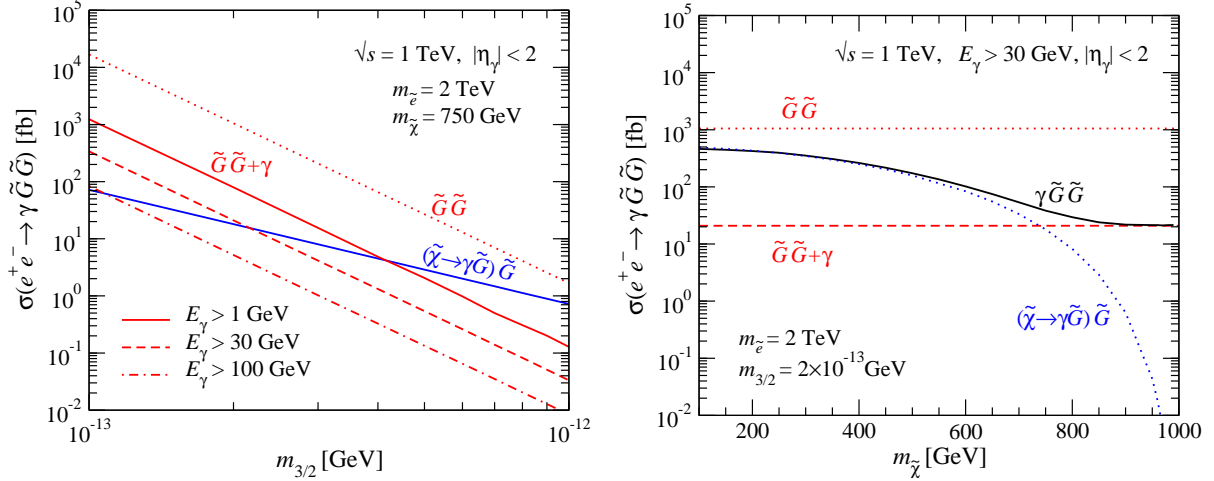


Fig. 4. Total cross sections of $e^+e^- \rightarrow \gamma\tilde{G}\tilde{G}$ as a function of the gravitino mass (left) and the neutralino mass (right) for $m_{\tilde{e}_{\pm}} = 2$ TeV at $\sqrt{s} = 1$ TeV. The contributions of the gravitino pair production and the neutralino-gravitino associated production are separately shown by red and blue lines, respectively. The cross section of $e^+e^- \rightarrow \tilde{G}\tilde{G}$ is also shown by a red dotted line as a reference. On the left plot the contributions of the $\tilde{G}\tilde{G}$ production are shown with different photon energy cuts $E_\gamma > 1, 30$ and 100 GeV, while the E_γ cut is fixed at 30 GeV on the right.

the decaying neutralino. The partial decay width for a photino-like neutralino is given by

$$\Gamma(\tilde{\chi} \rightarrow \gamma\tilde{G}) = \frac{m_{\tilde{\chi}}^5}{16\pi F^2}. \quad (19)$$

For instance, for $m_{\tilde{\chi}} = 750$ GeV and $m_{3/2} = 2 \times 10^{-13}$ GeV (i.e. $\sqrt{F} \approx 918$ GeV), the width is 6.6 GeV. With the neutralino being the NLSP, the branching ratio is unity, $B(\tilde{\chi} \rightarrow \gamma\tilde{G}) = 1$.

3.3 Physics parameters

To examine a viable SUSY parameter space for the $\gamma + \cancel{E}$ signal at future e^+e^- colliders, we present in Fig. 4 the total cross sections of $e^+e^- \rightarrow \gamma\tilde{G}\tilde{G}$ at $\sqrt{s} = 1$ TeV as a function of the gravitino mass (left) and the neutralino mass (right), where we fix the left- and right-handed selectron masses at 2 TeV. The representative Feynman diagrams for the process are depicted in Fig. 3. The contributions of the $\tilde{G}\tilde{G}$ and $\tilde{\chi}\tilde{G}$ productions are separately shown by red and blue lines, respectively.

As discussed in (14) and (18) and shown in the left plot in Fig. 4, the cross sections of the both subprocesses strongly depend on the gravitino mass.

The monophoton signal from the gravitino pair ($\tilde{G}\tilde{G} + \gamma$) is suppressed by the QED coupling α with respect to

the two-to-two process and strongly depends on the kinematical cuts due to the soft and collinear singularity of the initial state radiation. The cut dependence on the photon energy is presented in the left plot in Fig. 4. On the other hand, since the energy of the photons coming from the neutralino decay is restricted as

$$\frac{m_{\tilde{\chi}}^2}{2\sqrt{s}} < E_\gamma < \frac{\sqrt{s}}{2}, \quad (20)$$

the signal of $\tilde{\chi}\tilde{G}$ is not affected by the lower cuts on the photon energy unless the neutralino is light.

In the following, we impose the minimal cuts for the detection of photons as

$$E_\gamma > 0.03\sqrt{s}, \quad |\eta_\gamma| < 2, \quad (21)$$

and fix the gravitino mass at 2×10^{-13} GeV, which lies above the current exclusion limit by the jet+ \cancel{E} search at the LHC for the gravitino production in association with a gluino or a squark with masses around 500 GeV [11].^{5 6}

The right plot of Fig. 4 shows the neutralino mass dependence of the full signal cross section with the minimal

⁵ Astrophysics observables, e.g. energy losses of red giant stars [52] and supernova [53] can also provide the lower limit on the gravitino mass. But their limits are less stringent.

⁶ As discussed in Sect. 3.1, reliability of the effective theory calculation can also constrain the model parameter space.

cuts (21). While the $\tilde{G}\tilde{G}$ contribution is independent of the neutralino mass, the contribution from the $\tilde{\chi}\tilde{G}$ production is strongly suppressed when the neutralino mass approaches the CM energy due to the phase space closure. Therefore, the dominant subprocess can be different for different neutralino masses, giving rise to distinctive photon spectra. It should be noted that the interference between the two subprocesses is very small unless the neutralino width is too large. We verified this numerically by computing the two subprocess separately and checking that the sum of those reproduces the full $e^+e^- \rightarrow \gamma\tilde{G}\tilde{G}$ cross section, as in the figure. We suppress a possible contribution from the sgoldstinos by taking their masses to be too heavy to be produced on-shell.⁷ We note that, if those are lighter than the e^+e^- collision energy, the sgoldstino production in association with a photon and the subsequent decay contributes to the $\gamma\tilde{G}\tilde{G}$ final state. In Appendix B we briefly discuss the effect of sgoldstinos in the $\gamma\gamma \rightarrow \tilde{G}\tilde{G}$ process.

In the following, we focus on three different neutralino masses which exemplify different distributions. First, we fix the neutralino mass at 750 GeV so that $\sigma(\tilde{\chi}\tilde{G}) \sim \sigma(\tilde{G}\tilde{G} + \gamma)$. We subsequently take a lighter (heavier) neutralino at 650 (850) GeV so that the $\tilde{\chi}\tilde{G}$ ($\tilde{G}\tilde{G}$) production is dominant.

3.4 Technical setup and validation

Before moving to the simulation, let us comment on our model implementation and the validation. As mentioned in Sect. 1, the current MADGRAPH 5 (v2.0.2) [25] does not support four-fermion vertices involving more than one Majorana particle, and hence does not accept our UFO model file [46, 47] generated with FEYNRULES [23]. Therefore, first, we modified MADGRAPH 5 to allow us to import the model. Second, after generating the process, the corresponding four-point contact amplitudes should be modified by hand to have correct fermion flows. We have explicitly checked our numerical results of the total and differential cross sections by comparing with the analytic results for the two-to-two process in Sect. 3.1 as well as for the two-to-three process in the low-energy limit, $\sqrt{s} \ll m_{\tilde{e}, \tilde{\chi}, S, P}$, given in [19]. We have also checked precise agreements for the $\tilde{\chi}\tilde{G}$ process with the previous model implementations [27, 29, 31], which are constructed based on the effective gravitino Lagrangian in terms of the component fields, i.e. not by using the superspace module. We note that our model implementation allows us to generate different contributing processes, i.e. $\tilde{G}\tilde{G}$ and $\tilde{\chi}\tilde{G}$, within one event simulation.

4 Monophoton plus missing energy

We now perform the simulation of monophoton events with missing energy for a future e^+e^- collider. An irre-

ducible SM background comes from $e^+e^- \rightarrow \gamma\nu\bar{\nu}$. To remove contributions from $e^+e^- \rightarrow \gamma Z \rightarrow \gamma\nu\bar{\nu}$, we impose the Z-peak cut

$$E_\gamma < \frac{s - m_Z^2}{2\sqrt{s}} - 5\Gamma_Z, \quad (22)$$

in addition to the minimal cuts (21). The background from the t -channel W -exchange process, which is the most significant one, can be efficiently reduced by using a positively polarized e^- beam and a negatively polarized e^+ beam.

In Table 2, the signal cross sections of each subprocess, $\tilde{\chi}\tilde{G}$ and $\tilde{G}\tilde{G}$, as well as the SM background at $\sqrt{s} = 1$ TeV are presented without and with polarized e^\pm beams, where we take the beam polarization P_{e^\pm} ($|P_{e^\pm}| \leq 1$) as⁸

$$(P_{e^-}, P_{e^+}) = (0.9, -0.6), \quad (23)$$

and apply the kinematical cuts of (21) and (22). For the SUSY signal, we take the three benchmark neutralino masses with the gravitino mass fixed at 2×10^{-13} GeV for $m_{\tilde{e}} = 1$ and 2 TeV. As discussed in the previous section, heavier selectrons give the higher cross sections of the both subprocesses. Since the signal cross section with e^\pm beam polarizations is given by

$$\sigma(P_{e^-}, P_{e^+}) = 2 \sum_{\lambda_1} \left(\frac{1 + P_{e^-} \lambda_1}{2} \right) \left(\frac{1 - P_{e^+} \lambda_1}{2} \right) \sigma_{\lambda_1}, \quad (24)$$

the signal cross sections are enhanced by a factor of 1.54 with the above polarizations. On the other hand, the SM background is significantly reduced.

Figure 5 presents the photon energy E_γ (left) and rapidity η_γ (right) distributions for the three signal benchmarks and for the SM background. The signal energy spectra show two distinct features. First, there is a peak in the low-energy region which arises from the $\tilde{G}\tilde{G}$ production process since the initial state radiation is dominant as in the SM background. We also note that the low-energy spectra are independent of the neutralino mass. Second, there is a flat contribution in the high-energy region coming from $\tilde{\chi}\tilde{G}$ production, reflecting the isotropic neutralino decay. The contribution becomes smaller for the heavier neutralino (see also Table 2), and the lower edge allows us to extract the neutralino mass from (20).

The rapidity distributions are distinctive between the signal and the SM background. The photon coming from $\tilde{G}\tilde{G}$ production gives a flat η_γ distribution while the photon coming from the neutralino decay results in the central region (see [17] for a detailed discussion of the selectron mass dependence). In contrast, the photons of the SM background are emitted in the forward region.

Finally, we discuss the selectron mass dependence of the low-energy peak, which arises purely from $\tilde{G}\tilde{G}$ production. As discussed in Sect. 3.1, the total rate of the

⁷ We note that sgoldstinos with masses much smaller than the selectron mass do not obey a naturalness criterion [54].

⁸ $|P_{e^-}| > 0.8$ and $|P_{e^+}| > 0.5$ are designed at the International Linear Collider (ILC) [55].

Table 2. Cross sections in fb unit of each subprocess for the signal $e^+e^- \rightarrow \gamma\tilde{G}\tilde{G}$ and of the SM background $e^+e^- \rightarrow \gamma\nu\bar{\nu}$ at $\sqrt{s} = 1$ TeV, without and with beam polarizations. The kinematical cuts of (21) and (22) are applied. For the signal three (two) different neutralino (selectron) masses are taken with the gravitino mass fixed at 2×10^{-13} GeV.

(P_{e^-}, P_{e^+})	$m_{\tilde{\chi}} [\text{GeV}]$	$(m_{\tilde{e}} = 1 \text{ TeV})$		$(m_{\tilde{e}} = 2 \text{ TeV})$		SM bkg [fb]
		$\tilde{\chi}\tilde{G}$	$\tilde{G}\tilde{G}$	$\tilde{\chi}\tilde{G}$	$\tilde{G}\tilde{G}$	
(0, 0)	650	19.7		49.2		1452
	750	6.0	10.4	15.8	21.1	
	850	1.0		2.5		
(0.9, -0.6)	650	30.4		75.8		64.9
	750	9.2	16.1	24.3	32.7	
	850	1.5		3.4		

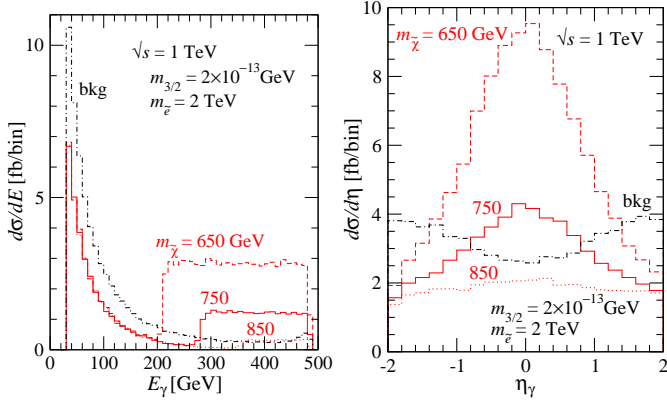


Fig. 5. Photon energy (left) and rapidity (right) distributions for $e^+e^- \rightarrow \gamma\tilde{G}\tilde{G}$ at $\sqrt{s} = 1$ TeV for different neutralino masses with $m_{3/2} = 2 \times 10^{-13}$ GeV and $m_{\tilde{e}\pm} = 2$ TeV. The kinematical cuts in (21) and (22) as well as the beam polarizations in (23) are applied. The SM background is also shown.

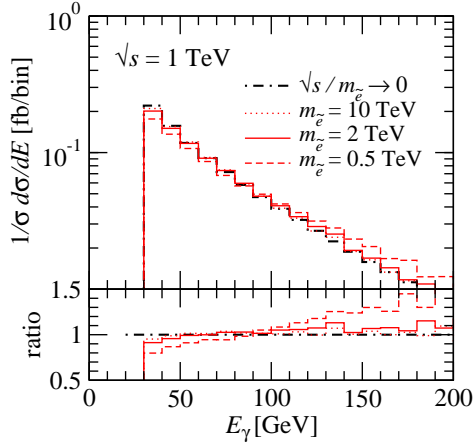


Fig. 6. Normalized photon energy distributions for $e^+e^- \rightarrow \gamma\tilde{G}\tilde{G}$ at $\sqrt{s} = 1$ TeV for $m_{\tilde{e}\pm} = 0.5, 2, 10$ TeV and for the high-mass limit, where the kinematical cuts (21) are applied. The ratios to the case in the high-mass limit are also shown.

$e^+e^- \rightarrow \tilde{G}\tilde{G}$ process depends on the selectron masses. In addition, the photon spectrum becomes harder for lighter selectrons; see Fig. 6, where we show the normalized photon energy distributions for $m_{\tilde{e}\pm} = 0.5, 2, 10$ TeV and for the $\sqrt{s}/m_{\tilde{e}} = 0$ limit [19]. The distribution for $m_{\tilde{e}\pm} =$

10 TeV is in good agreement with the one in the high-mass limit. We note that in this limit the $e^+e^- \rightarrow \gamma\tilde{G}\tilde{G}$ differential cross section can be described by the $e^+e^- \rightarrow \tilde{G}\tilde{G}$ cross section times the standard photon splitting function in a good approximation [19].

5 Summary

Direct gravitino productions can be observed in current and future collider experiments if the gravitino is very light. In this article, we revisited gravitino pair production and neutralino-gravitino associated production, and studied the $\gamma + \cancel{E}$ signal for future e^+e^- colliders.

By using the superspace formalism, we constructed a simple SUSY QED model that allows us to study the parameter space for the both processes, and implemented the model in the FEYNRULES and MADGRAPH 5 frameworks. We note that special implementations are needed to treat the Majorana four-fermion interaction in MADGRAPH 5.

We discussed the parameter dependence of the signal cross sections in detail, and showed that the relative importance between the two signal processes varies with the gravitino and neutralino masses as well as with kinematical cuts.

We performed the event simulation for the SUSY signal as well as the SM background, taking into account the signal selection cut and the beam polarizations, and showed that the photon spectra from the two subprocesses are very distinctive. This is because the photon coming from the $\tilde{G}\tilde{G}$ production is mostly initial state radiation, while the $\tilde{\chi}\tilde{G}$ associated production process leads to an energetic photon from the neutralino decay. We expect that future e^+e^- colliders could explore the parameter space around our benchmark points and hence provide information on the masses of the relevant SUSY particles as well as the SUSY breaking scale.

Before closing, we note that the extension of our simple SUSY QED model to the general MSSM is straightforward, which is applicable for hadron colliders.

Acknowledgments

We wish to thank B. Fuks and O. Mattelaer for their help with FEYNRULES and MADGRAPH5 and F. Maltoni and C. Petersson for useful discussions. We also thank Y. Takaesu and

P. Tziveloglou for helpful discussions and comments on the draft. This work has been supported in part by the Belgian Federal Science Policy Office through the Interuniversity Attraction Pole P7/37, and by the Strategic Research Program “High Energy Physics” and the Research Council of the Vrije Universiteit Brussel.

A Lagrangian in terms of the component fields

In Sect. 2 we gave the Lagrangian of our model in terms of the superfields. In this appendix, for completeness, we present the corresponding interaction Lagrangian in terms of the component fields. The relevant terms of the effective interaction Lagrangian among gravitinos (i.e. goldstinos) $\psi_{\tilde{G}}$ and fields in the visible sector, that is, right- and left-handed selectron $\phi_{\tilde{e}\pm}$, electron ψ_e , photino-like neutralino $\psi_{\tilde{\chi}}$,⁹ and photon A^μ are given in the four-component notation by

$$\begin{aligned} \mathcal{L}_{\tilde{G}} = & \mp \frac{im_{\tilde{e}\pm}^2}{F} (\bar{\psi}_{\tilde{G}} P_{\pm} \psi_e \phi_{\tilde{e}\pm}^* - \bar{\psi}_e P_{\mp} \psi_{\tilde{G}} \phi_{\tilde{e}\pm}) \\ & - \frac{m_{\tilde{\chi}}}{4\sqrt{2}F} \bar{\psi}_{\tilde{G}} [\gamma^\mu, \gamma^\nu] \psi_{\tilde{\chi}} F_{\mu\nu} \\ & - \frac{m_{\tilde{e}\pm}^2}{F^2} \bar{\psi}_e P_{\mp} \psi_{\tilde{G}} \bar{\psi}_{\tilde{G}} P_{\pm} \psi_e, \end{aligned} \quad (25)$$

where $P_{\pm} = \frac{1}{2}(1 \pm \gamma^5)$ is the chiral projection operator and $F_{\mu\nu} = \partial_\mu A_\nu - \partial_\nu A_\mu$ the photon field strength tensor. The interactions among sgoldstino $\phi = \frac{1}{\sqrt{2}}(\phi_S + i\phi_P)$ and gravitino or photon are given by

$$\begin{aligned} \mathcal{L}_{S,P} = & -\frac{m_\phi^2}{2\sqrt{2}F} \bar{\psi}_{\tilde{G}} (\phi_S + i\gamma^5 \phi_P) \psi_{\tilde{G}} \\ & + \frac{m_{\tilde{\chi}}}{2\sqrt{2}F} (\phi_S F^{\mu\nu} F_{\mu\nu} - \phi_P F^{\mu\nu} \tilde{F}_{\mu\nu}), \end{aligned} \quad (26)$$

where $\tilde{F}_{\mu\nu} = \frac{1}{2}\epsilon_{\mu\nu\alpha\beta} F^{\alpha\beta}$ is the dual tensor with $\epsilon_{0123} = +1$. All other relevant terms in the visible sector are

$$\begin{aligned} \mathcal{L}_{\text{vis}} = & g_e \bar{\psi}_e \gamma_\mu \psi_e A^\mu + ig_e (\phi_{\tilde{e}\pm}^* \overleftrightarrow{\partial}_\mu \phi_{\tilde{e}\pm}) A^\mu \\ & \mp \sqrt{2} g_e (\bar{\psi}_{\tilde{\chi}} P_{\pm} \psi_e \phi_{\tilde{e}\pm}^* + \bar{\psi}_e P_{\mp} \psi_{\tilde{\chi}} \phi_{\tilde{e}\pm}), \end{aligned} \quad (27)$$

where $g_e = \sqrt{4\pi\alpha}$ is the QED coupling constant.

We note that we follow the convention of the SUSY Les Houches accord [56] for the covariant derivative and the gaugino and gravitino field definitions. To translate our Lagrangian into the FEYNRULES convention, one has to change the coupling as $g_e \rightarrow -g_e$, and redefine the fields as $\psi_{\tilde{\chi}} \rightarrow -\psi_{\tilde{\chi}}$ and $\psi_{\tilde{G}} \rightarrow -\psi_{\tilde{G}}$.

⁹ See e.g. Appendix A in [31] for the general case of the neutralino mixing.

B Gravitino pair production in $\gamma\gamma$ collisions

In this article we assumed that the sgoldstinos are too heavy to be produced on-shell, and hence those are irrelevant to the $e^+e^- \rightarrow \gamma\tilde{G}\tilde{G}$ process. However, our model has no limitation to study processes involving sgoldstinos by construction in the superspace formalism. In this appendix, to validate our model implementation of sgoldstinos, we discuss gravitino pair production in $\gamma\gamma$ collisions, where the sgoldstinos play an important role for the unitarity [34, 35].¹⁰

Similar to Sect. 3.1, we present the helicity amplitude explicitly for the process

$$\gamma(p_1, \lambda_1) + \gamma(p_2, \lambda_2) \rightarrow \tilde{G}\left(p_3, \frac{\lambda_3}{2}\right) + \tilde{G}\left(p_4, \frac{\lambda_4}{2}\right), \quad (28)$$

where the four momenta (p_i) and helicities ($\lambda_i = \pm 1$) are defined in the center-of-mass (CM) frame of the $\gamma\gamma$ collision. As seen in Fig. 7, in our SUSY QED model, the helicity amplitudes are given by the sum of the s -channel scalar (S) and pseudoscalar (P) sgoldstino amplitudes and the t, u -channel photino-like neutralino exchange amplitudes:

$$\begin{aligned} \mathcal{M}_{\lambda_1\lambda_2, \lambda_3\lambda_4} = & \epsilon_\mu(p_1, \lambda_1) \epsilon_\nu(p_2, \lambda_2) \\ & \times (\mathcal{M}_{\lambda_3\lambda_4}^{S, \mu\nu} + \mathcal{M}_{\lambda_3\lambda_4}^{P, \mu\nu} + \mathcal{M}_{\lambda_3\lambda_4}^{t, \mu\nu} + \mathcal{M}_{\lambda_3\lambda_4}^{u, \mu\nu}), \end{aligned} \quad (29)$$

where the photon wavefunctions are factorized. Using the straightforward Feynman rules for Majorana fermions [48], the above amplitudes are written, based on the effective Lagrangian in Appendix A, as

$$\begin{aligned} i\mathcal{M}_{\lambda_3\lambda_4}^{S, \mu\nu} = & -\frac{im_{\tilde{\chi}}m_\phi^2}{F^2} \frac{1}{s - m_\phi^2} (p_1 \cdot p_2 g^{\mu\nu} - p_2^\mu p_1^\nu) \\ & \times \bar{u}(p_3, \lambda_3) v(p_4, \lambda_4), \end{aligned} \quad (30)$$

$$\begin{aligned} i\mathcal{M}_{\lambda_3\lambda_4}^{P, \mu\nu} = & -\frac{im_{\tilde{\chi}}m_\phi^2}{F^2} \frac{1}{s - m_\phi^2} \epsilon^{\mu\nu\alpha\beta} p_{2\alpha} p_{1\beta} \\ & \times \bar{u}(p_3, \lambda_3) i\gamma^5 v(p_4, \lambda_4), \end{aligned} \quad (31)$$

$$\begin{aligned} i\mathcal{M}_{\lambda_3\lambda_4}^{t, \mu\nu} = & -\frac{im_{\tilde{\chi}}^2}{8F^2} \frac{1}{t - m_{\tilde{\chi}}^2} \\ & \times \bar{u}(p_3, \lambda_3) [\gamma^\mu, \not{p}_1] (\not{p}_1 - \not{p}_3 - m_{\tilde{\chi}}) [\not{p}_2, \gamma^\nu] v(p_4, \lambda_4), \end{aligned} \quad (32)$$

$$\begin{aligned} i\mathcal{M}_{\lambda_3\lambda_4}^{u, \mu\nu} = & \frac{im_{\tilde{\chi}}^2}{8F^2} \frac{1}{u - m_{\tilde{\chi}}^2} \\ & \times \bar{u}(p_3, \lambda_3) [\gamma^\mu, \not{p}_2] (\not{p}_1 - \not{p}_4 + m_{\tilde{\chi}}) [\not{p}_1, \gamma^\nu] v(p_4, \lambda_4), \end{aligned} \quad (33)$$

where the common sgoldstino mass is taken as $m_{S,P} = m_\phi$. The reduced helicity amplitudes $\hat{\mathcal{M}}$ are defined as

$$\mathcal{M}_{\lambda_1\lambda_2, \lambda_3\lambda_4} = \frac{m_{\tilde{\chi}} s^{3/2}}{2F^2} \hat{\mathcal{M}}_{\lambda_1\lambda_2, \lambda_3\lambda_4}, \quad (34)$$

¹⁰ The amplitudes were calculated by using the explicit spin-3/2 gravitino wavefunction analytically in the high-energy limit in [34, 35] and numerically in [28], including the spin-2 graviton exchange diagram.

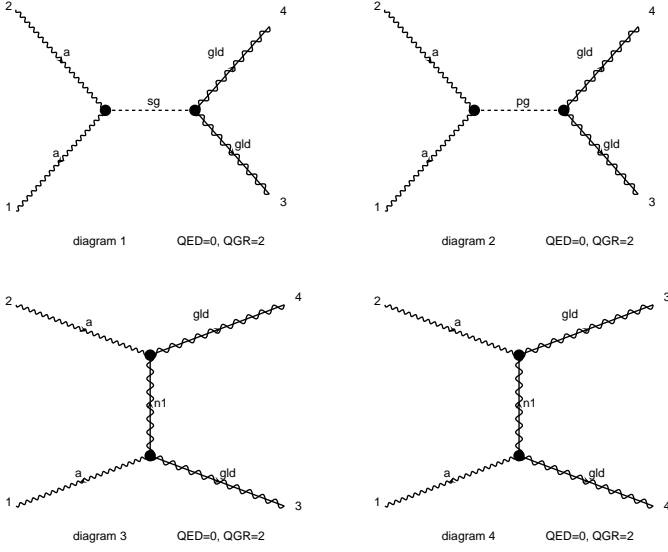


Fig. 7. Feynman diagrams for gravitino pair production in $\gamma\gamma$ collisions, generated by MADGRAPH 5 [25]. **gld**, **sg**, **pg**, and **n1** denote a gravitino, a scalar sgoldstino, a pseudoscalar sgoldstino, and a neutralino, respectively.

and presented in Table 3. The analytic expression for the total cross section can be found in [57], and our numerical results agree well with it.

Figure 8 shows the total cross sections as a function of the CM energy \sqrt{s} for $m_{\tilde{\chi}} = 0.5$ TeV (blue) and $m_{\tilde{\chi}} = 2$ TeV (red) with $m_{3/2} = 2 \times 10^{-13}$ GeV. First, let us consider the heavy sgoldstino case, $m_\phi = 100$ TeV. In the low-energy limit, $\sqrt{s} \ll m_{\phi, \tilde{\chi}}$, similar to the e^+e^- collision (15), the total cross section is given by [57]

$$\sigma = \frac{s^3}{640\pi F^4}, \quad (35)$$

shown by a black-solid line in Fig 8. Due to a cancellation between the sgoldstino and neutralino amplitudes for $\lambda_1 = \lambda_2 = -\lambda_3 = -\lambda_4$ as can be seen in Table 3, the dominant contribution is given by the amplitudes for $\lambda_1 = -\lambda_2$, which are proportional to s^2 in the low-energy limit. To emphasize the importance of the interference, the contribution without the sgoldstino amplitudes is also shown by a dotted line in Fig. 8. On the other hand, in the case where the neutralino mass is smaller than the CM energy, $m_{\tilde{\chi}} \ll \sqrt{s} \ll m_\phi$, the cross section is dominated by the sgoldstino contributions and deviates from the one in the low-energy limit.

We now turn to the case where the sgoldstinos are relatively light, $m_\phi = 1$ TeV. In our SUSY QED model, the partial decay width of the sgoldstinos are given by [58]

$$\Gamma(S, P \rightarrow \tilde{G}\tilde{G}) = \frac{m_\phi^5}{32\pi F^2}, \quad (36)$$

$$\Gamma(S, P \rightarrow \gamma\gamma) = \frac{m_{\tilde{\chi}}^2 m_\phi^3}{32\pi F^2}. \quad (37)$$

For $m_\phi = 1$ TeV and $m_{3/2} = 2 \times 10^{-13}$ GeV (i.e. $\sqrt{F} \approx 918$ GeV), the width for a gravitino pair is 14.0 GeV and

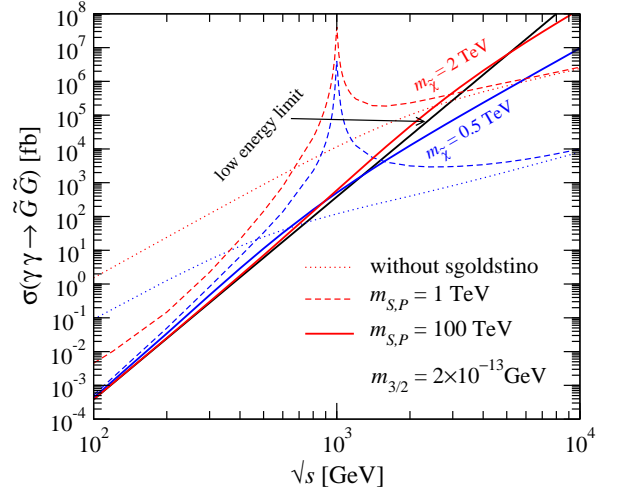


Fig. 8. Total cross sections of $\gamma\gamma \rightarrow \tilde{G}\tilde{G}$ as a function of the collision energy for $m_{3/2} = 2 \times 10^{-13}$ GeV. The sgoldstino masses are taken to be 1 TeV (dashed) and 100 TeV (solid), while the neutralino mass is fixed at 0.5 TeV (blue) and 2 TeV (red). We also show the cross section in the low energy limit (black solid) as well as the contributions without the sgoldstino interactions (dotted).

for a photon pair is 3.5 (55.9) GeV for $m_{\tilde{\chi}} = 0.5$ (2) TeV. For the $m_{\tilde{\chi}} = 2$ TeV case, the finite width effect can be seen as a deviation from the cross section (35) in the low-energy region in Fig. 8. For $\sqrt{s} \approx m_\phi$, one can clearly see the resonant peak. In the high-energy limit, $\sqrt{s} \gg m_{\phi, \tilde{\chi}}$, the cross section approaches the value obtained by neglecting the sgoldstino amplitudes, since the $\lambda_1 = -\lambda_2$ amplitudes become dominant; see Table 3.

Finally, we note that collider signatures of sgoldstinos have been studied in [58–69], and our model file can be also applied for such sgoldstino phenomenology.

References

1. **OPAL** Collaboration, G. Abbiendi et al., *Photonic events with missing energy in e^+e^- collisions at $\sqrt{s} = 189$ GeV*, *Eur.Phys.J.* **C18** (2000) 253–272, [[hep-ex/0005002](#)].
2. **ALEPH** Collaboration, A. Heister et al., *Single photon and multiphoton production in e^+e^- collisions at \sqrt{s} up to 209 GeV*, *Eur.Phys.J.* **C28** (2003) 1–13.
3. **L3** Collaboration, P. Achard et al., *Single photon and multiphoton events with missing energy in e^+e^- collisions at LEP*, *Phys.Lett.* **B587** (2004) 16–32, [[hep-ex/0402002](#)].
4. **DELPHI** Collaboration, J. Abdallah et al., *Photon events with missing energy in e^+e^- collisions at $\sqrt{s} = 130$ GeV to 209 GeV*, *Eur.Phys.J.* **C38** (2005) 395–411, [[hep-ex/0406019](#)].
5. **CDF** Collaboration, D. Acosta et al., *Limits on extra dimensions and new particle production in the exclusive photon and missing energy signature in $p\bar{p}$ collisions at $\sqrt{s} = 1.8$ TeV*, *Phys.Rev.Lett.* **89** (2002) 281801, [[hep-ex/0205057](#)].
6. **D0** Collaboration, V. Abazov et al., *Search for large extra dimensions via single photon plus missing energy*

Table 3. The reduced helicity amplitudes $\hat{\mathcal{M}}_{\lambda_1\lambda_2,\lambda_3\lambda_4}$ defined in (34) for $\gamma_{\lambda_1}\gamma_{\lambda_2} \rightarrow \tilde{G}_{\lambda_3}\tilde{G}_{\lambda_4}$.

$\lambda_1\lambda_2\lambda_3\lambda_4$	$\hat{\mathcal{M}}^S$	$\hat{\mathcal{M}}^P$	$\hat{\mathcal{M}}^t$	$\hat{\mathcal{M}}^u$
$\pm\pm\pm\pm$	$\mp\left[\frac{m_\phi^2}{s-m_\phi^2} - \frac{m_\phi^2}{s-m_\phi^2}\right]$			
$\pm\pm\mp\mp$	$\pm\left[\frac{m_\phi^2}{s-m_\phi^2} + \frac{m_\phi^2}{s-m_\phi^2}\right]$		$-\frac{m_{\tilde{\chi}}^2}{t-m_{\tilde{\chi}}^2}(1-\cos\theta)$	$-\frac{m_{\tilde{\chi}}^2}{u-m_{\tilde{\chi}}^2}(1+\cos\theta)$
$\pm\mp\pm\mp$				$\frac{m_{\tilde{\chi}}\sqrt{s}}{(u-m_{\tilde{\chi}}^2)}\frac{1}{2}(1+\cos\theta)\sin\theta$
$\pm\mp\mp\pm$			$-\frac{m_{\tilde{\chi}}\sqrt{s}}{(t-m_{\tilde{\chi}}^2)}\frac{1}{2}(1-\cos\theta)\sin\theta$	

- final states at $\sqrt{s} = 1.96$ TeV, *Phys.Rev.Lett.* **101** (2008) 011601, [arXiv:0803.2137].
7. **CDF** Collaboration, T. Aaltonen et al., *Search for large extra dimensions in final states containing one photon or jet and large missing transverse energy produced in $p\bar{p}$ collisions at $\sqrt{s} = 1.96$ TeV*, *Phys.Rev.Lett.* **101** (2008) 181602, [arXiv:0807.3132].
 8. **CMS** Collaboration, S. Chatrchyan et al., *Search for Dark Matter and Large Extra Dimensions in pp Collisions Yielding a Photon and Missing Transverse Energy*, *Phys.Rev.Lett.* **108** (2012) 261803, [arXiv:1204.0821].
 9. **ATLAS** Collaboration, G. Aad et al., *Search for dark matter candidates and large extra dimensions in events with a photon and missing transverse momentum in pp collision data at $\sqrt{s} = 7$ TeV with the ATLAS detector*, *Phys.Rev.Lett.* **110** (2013) 011802, [arXiv:1209.4625].
 10. **CDF** Collaboration, T. Affolder et al., *Limits on gravitino production and new processes with large missing transverse energy in $p\bar{p}$ collisions at $\sqrt{s} = 1.8$ TeV*, *Phys.Rev.Lett.* **85** (2000) 1378–1383, [hep-ex/0003026].
 11. **ATLAS** Collaboration, *Search for New Phenomena in Monojet plus Missing Transverse Momentum Final States using 10 fb^{-1} of pp Collisions at $\sqrt{s} = 8$ TeV with the ATLAS detector at the LHC*, ATLAS-CONF-2012-147 (2012).
 12. P. Fayet, *Lower Limit on the Mass of a Light Gravitino from e^+e^- Annihilation Experiments*, *Phys.Lett.* **B175** (1986) 471.
 13. D. A. Dicus, S. Nandi, and J. Woodside, *A New source of single photons from Z^0 decay*, *Phys.Lett.* **B258** (1991) 231–235.
 14. J. L. Lopez, D. V. Nanopoulos, and A. Zichichi, *Supersymmetric photonic signals at LEP*, *Phys.Rev.Lett.* **77** (1996) 5168–5171, [hep-ph/9609524].
 15. J. L. Lopez, D. V. Nanopoulos, and A. Zichichi, *Single photon signals at LEP in supersymmetric models with a light gravitino*, *Phys.Rev.* **D55** (1997) 5813–5825, [hep-ph/9611437].
 16. S. Baek, S. C. Park, and J.-h. Song, *Kaluza-Klein gravitino production with a single photon at e^+e^- colliders*, *Phys.Rev.* **D66** (2002) 056004, [hep-ph/0206008].
 17. K. Mawatari, B. Oexl, and Y. Takaesu, *Associated production of light gravitinos in e^+e^- and $e^-\gamma$ collisions*, *Eur.Phys.J.* **C71** (2011) 1783, [arXiv:1106.5592].
 18. O. Nachtmann, A. Reiter, and M. Wirbel, *Single Jet and Single Photon Production in Proton - Anti-proton Collisions and e^+e^- Annihilation in a Supersymmetric Model*, *Z.Phys.* **C27** (1985) 577.
 19. A. Brignole, F. Feruglio, and F. Zwirner, *Signals of a superlight gravitino at e^+e^- colliders when the other superparticles are heavy*, *Nucl.Phys.* **B516** (1998) 13–28, [hep-ph/9711516].
 20. A. Brignole, F. Feruglio, M. L. Mangano, and F. Zwirner, *Signals of a superlight gravitino at hadron colliders when the other superparticles are heavy*, *Nucl.Phys.* **B526** (1998) 136–152, [hep-ph/9801329].
 21. N. D. Christensen and C. Duhr, *FeynRules - Feynman rules made easy*, *Comput.Phys.Comm.* **180** (2009) 1614–1641, [arXiv:0806.4194].
 22. C. Duhr and B. Fuks, *A superspace module for the FeynRules package*, *Comput.Phys.Comm.* **182** (2011) 2404–2426, [arXiv:1102.4191].
 23. A. Alloul, N. D. Christensen, C. Degrande, C. Duhr, and B. Fuks, *FeynRules 2.0 - A complete toolbox for tree-level phenomenology*, *Comput.Phys.Comm.* **185** (2014) 2250–2300, [arXiv:1310.1921].
 24. J. Alwall, P. Demin, S. de Visscher, R. Frederix, M. Herquet, et al., *MadGraph/MadEvent v4: The New Web Generation*, *JHEP* **0709** (2007) 028, [arXiv:0706.2334].
 25. J. Alwall, M. Herquet, F. Maltoni, O. Mattelaer, and T. Stelzer, *MadGraph 5 : Going Beyond*, *JHEP* **1106** (2011) 128, [arXiv:1106.0522].
 26. K. Hagiwara, K. Mawatari, and Y. Takaesu, *HELAS and MadGraph with spin-3/2 particles*, *Eur.Phys.J.* **C71** (2011) 1529, [arXiv:1010.4255].
 27. K. Mawatari and Y. Takaesu, *HELAS and MadGraph with goldstinos*, *Eur.Phys.J.* **C71** (2011) 1640, [arXiv:1101.1289].
 28. N. D. Christensen, P. de Aquino, N. Deutschmann, C. Duhr, B. Fuks, et al., *Simulating spin- $\frac{3}{2}$ particles at colliders*, *Eur.Phys.J.* **C73** (2013) 2580, [arXiv:1308.1668].
 29. R. Argurio, K. De Causmaecker, G. Ferretti, A. Mariotti, K. Mawatari, et al., *Collider signatures of goldstini in gauge mediation*, *JHEP* **1206** (2012) 096, [arXiv:1112.5058].
 30. P. de Aquino, F. Maltoni, K. Mawatari, and B. Oexl, *Light Gravitino Production in Association with Gluinos at the LHC*, *JHEP* **1210** (2012) 008, [arXiv:1206.7098].
 31. K. Mawatari, *Associated production of light gravitinos at future linear colliders*, arXiv:1202.0507.
 32. J. D'Hondt, K. De Causmaecker, B. Fuks, A. Mariotti, K. Mawatari, et al., *Multilepton signals of gauge mediated supersymmetry breaking at the LHC*, *Phys.Lett.* **B731** (2014) 7–12, [arXiv:1310.0018].

33. G. Ferretti, A. Mariotti, K. Mawatari, and C. Petersson, *Multiphoton signatures of goldstini at the LHC*, *JHEP* **1404** (2014) 126, [[arXiv:1312.1698](#)].
34. T. Bhattacharya and P. Roy, *Role of Chiral Scalar and Pseudoscalar in Two Photon Production of a Superlight Gravitino*, *Phys.Rev.* **D38** (1988) 2284.
35. T. Bhattacharya and P. Roy, *TREE UNITARITY IN BROKEN SUPERGRAVITY. 2. DOUBLE GRAVITINO AMPLITUDE*, *Nucl.Phys.* **B328** (1989) 481.
36. M. A. Luty and E. Ponton, *Effective Lagrangians and light gravitino phenomenology*, *Phys.Rev.* **D57** (1998) 4167–4173, [[hep-ph/9706268](#)].
37. A. Brignole, F. Feruglio, and F. Zwirner, *On the effective interactions of a light gravitino with matter fermions*, *JHEP* **9711** (1997) 001, [[hep-th/9709111](#)].
38. T. Clark, T. Lee, S. Love, and G.-H. Wu, *On the interactions of light gravitinos*, *Phys.Rev.* **D57** (1998) 5912–5915, [[hep-ph/9712353](#)].
39. A. Brignole, J. Casas, J. Espinosa, and I. Navarro, *Low scale supersymmetry breaking: Effective description, electroweak breaking and phenomenology*, *Nucl.Phys.* **B666** (2003) 105–143, [[hep-ph/0301121](#)].
40. R. Casalbuoni, S. De Curtis, D. Dominici, F. Feruglio, and R. Gatto, *A GRAVITINO - GOLDSTINO HIGH-ENERGY EQUIVALENCE THEOREM*, *Phys.Lett.* **B215** (1988) 313.
41. R. Casalbuoni, S. De Curtis, D. Dominici, F. Feruglio, and R. Gatto, *High-Energy Equivalence Theorem in Spontaneously Broken Supergravity*, *Phys.Rev.* **D39** (1989) 2281.
42. D. Volkov and V. Soroka, *Higgs Effect for Goldstone Particles with Spin 1/2*, *JETP Lett.* **18** (1973) 312–314.
43. S. Deser and B. Zumino, *Broken Supersymmetry and Supergravity*, *Phys.Rev.Lett.* **38** (1977) 1433.
44. S. Ambrosanio, G. L. Kane, G. D. Kribs, S. P. Martin, and S. Mrenna, *Search for supersymmetry with a light gravitino at the Fermilab Tevatron and CERN LEP colliders*, *Phys.Rev.* **D54** (1996) 5395–5411, [[hep-ph/9605398](#)].
45. I. Antoniadis, E. Dudas, D. Ghilencea, and P. Tziveloglou, *Non-linear MSSM*, *Nucl.Phys.* **B841** (2010) 157–177, [[arXiv:1006.1662](#)].
46. C. Degrande, C. Duhr, B. Fuks, D. Grellscheid, O. Mattelaer, et al., *UFO - The Universal FeynRules Output*, *Comput.Phys.Comm.* **183** (2012) 1201–1214, [[arXiv:1108.2040](#)].
47. P. de Aquino, W. Link, F. Maltoni, O. Mattelaer, and T. Stelzer, *ALOHA: Automatic Libraries Of Helicity Amplitudes for Feynman Diagram Computations*, *Comput.Phys.Comm.* **183** (2012) 2254–2263, [[arXiv:1108.2041](#)].
48. A. Denner, H. Eck, O. Hahn, and J. Kublbeck, *Feynman rules for fermion number violating interactions*, *Nucl.Phys.* **B387** (1992) 467–484.
49. P. Checchia, *Sensitivity to the gravitino mass from single photon spectrum at TESLA linear collider*, [hep-ph/9911208](#).
50. S. Gopalakrishna, M. Perelstein, and J. D. Wells, *Extra dimensions versus supersymmetric interpretation of missing energy events at a linear collider*, *eConf* **C010630** (2001) P311, [[hep-ph/0110339](#)].
51. C. Petersson, A. Romagnoni, and R. Torre, *Higgs Decay with Monophoton + MET Signature from Low Scale Supersymmetry Breaking*, *JHEP* **1210** (2012) 016, [[arXiv:1203.4563](#)].
52. M. Fukugita and N. Sakai, *ASTROPHYSICAL CONSTRAINTS ON BROKEN SUPERSYMMETRY*, *Phys.Lett.* **B114** (1982) 23.
53. D. A. Dicus, R. N. Mohapatra, and V. L. Teplitz, *Supernova constraints on a superlight gravitino*, *Phys.Rev.* **D57** (1998) 578–582, [[hep-ph/9708369](#)].
54. A. Brignole, F. Feruglio, and F. Zwirner, *Four-fermion interactions and sgoldstino masses in models with a superlight gravitino*, *Phys.Lett.* **B438** (1998) 89–95, [[hep-ph/9805282](#)].
55. ILC Collaboration, J. Brau et al., *ILC Reference Design Report: ILC Global Design Effort and World Wide Study*, [arXiv:0712.1950](#).
56. P. Z. Skands, B. Allanach, H. Baer, C. Balazs, G. Belanger, et al., *SUSY Les Houches accord: Interfacing SUSY spectrum calculators, decay packages, and event generators*, *JHEP* **0407** (2004) 036, [[hep-ph/0311123](#)].
57. A. Brignole, F. Feruglio, and F. Zwirner, *Aspects of spontaneously broken $N=1$ global supersymmetry in the presence of gauge interactions*, *Nucl.Phys.* **B501** (1997) 332–374, [[hep-ph/9703286](#)].
58. E. Perazzi, G. Ridolfi, and F. Zwirner, *Signatures of massive sgoldstinos at e^+e^- colliders*, *Nucl.Phys.* **B574** (2000) 3–22, [[hep-ph/0001025](#)].
59. D. A. Dicus and P. Roy, *Restrictions on Gravitino Mass From Chiral Scalar and Pseudoscalar Production*, *Phys.Rev.* **D42** (1990) 938–940.
60. E. Perazzi, G. Ridolfi, and F. Zwirner, *Signatures of massive sgoldstinos at hadron colliders*, *Nucl.Phys.* **B590** (2000) 287–305, [[hep-ph/0005076](#)].
61. D. Gorbunov, *Light sgoldstino: Precision measurements versus collider searches*, *Nucl.Phys.* **B602** (2001) 213–237, [[hep-ph/0007325](#)].
62. D. Gorbunov, V. Ilyin, and B. Mele, *Sgoldstino events in top decays at LHC*, *Phys.Lett.* **B502** (2001) 181–188, [[hep-ph/0012150](#)].
63. DELPHI Collaboration, P. Abreu et al., *Search for the sgoldstino at \sqrt{s} from 189 GeV to 202 GeV*, *Phys.Lett.* **B494** (2000) 203–214, [[hep-ex/0102044](#)].
64. P. Checchia and E. Piotto, *Sensitivity to sgoldstino states at the future linear e^+e^- and photon colliders*, [hep-ph/0102208](#).
65. D. S. Gorbunov and A. V. Semenov, *CompHEP package with light gravitino and sgoldstinos*, [hep-ph/0111291](#).
66. D. Gorbunov and N. Krasnikov, *Prospects for sgoldstino search at the LHC*, *JHEP* **0207** (2002) 043, [[hep-ph/0203078](#)].
67. S. Demidov and D. Gorbunov, *LHC prospects in searches for neutral scalars in $pp \rightarrow \gamma\gamma + \text{jet}$: SM Higgs boson, radion, sgoldstino*, *Phys.Atom.Nucl.* **69** (2006) 712–720, [[hep-ph/0405213](#)].
68. C. Petersson and A. Romagnoni, *The MSSM Higgs Sector with a Dynamical Goldstino Supermultiplet*, *JHEP* **1202** (2012) 142, [[arXiv:1111.3368](#)].
69. B. Bellazzini, C. Petersson, and R. Torre, *Photophilic Higgs from sgoldstino mixing*, *Phys.Rev.* **D86** (2012) 033016, [[arXiv:1207.0803](#)].